In this chapter, we present a comparative study of polyaniline/polysaccharide composites (starch, carboxymethyl cellulose, cellulose acetate, and chitosan) by FTIR, UV-Visible, SEM and electrochemical analysis. We proposed that simultaneously three different phenomena happen while formation of composite system that may be listed as degradation of polysaccharide, polymerization of aniline, the formation of polyaniline-polysaccharide composite. Effects of hydrochloric acid and oxidizing agent APS (ammonium peroxydisulphate) on the structure of polysaccharides were also investigated. We obtained dissimilar product yield and variable polyaniline and polysaccharide ratio in the composite system even though experimental conditions were same. The possible reasons responsible for the observed differences as well as characteristics and morphology of protonated and deprotonated composite materials are discussed.

4.1. Introduction:

PANI based composite materials have been prepared along with other class of materials such as described in chapter 2. Studies of optical, electrical, morphological, mechanical, spectroscopic and thermal properties of a composite material are of great importance to understand its behavior and possibility of application of the material in a desired field (Syed et al. 1991; Zhao et al. 2011; Khan et al. 2012; Dhand et al. 2011).

Most of the polysaccharides are abundantly obtained from natural resources mainly plants. Thus, the major sources of starch for the use of human beings are the cereals but roots and tubers are also important (Daniel et al. 2001; Tester et al. 2002). Cellulose is the most abundant renewable natural polymer material that is an inexhaustible resource. Carboxymethyl cellulose is a water soluble derivative of cellulose, consisting of β-(1→4) glucopyranose residues; it is biodegradable, biocompatible, resistant to oil grease and

solvents, etc. (Wang et al. 2005). Cellulose acetate is an odorless, colorless, tough, and durable material with high structural strength and melting point; its low reactivity to organic materials can be enhanced by high flexural and tensile strength of natural fibers (BeMiller et al. 2001). Chitosan composed of randomly distributed (1→4)-linked 2-amino-2-deoxy-s-D-glucan is used as a seed treatment material, bio-pesticide, anti-fungal agent, absorbent, bandages to reduce bleeding, an antibacterial agent, drug deliver drugs and immobilization of enzymes (Stephen et al. 2011).

Interesting motivational aspects to carried out this research work are; to enhance our understanding about the interactions between the building block of polysaccharides (sugar or derived sugar molecular structures) with polyaniline chain, to explain the observed variation in structural morphology in terms of chemical interaction, to establish correlation of other properties/parameters/characteristics with the different stretching and bending vibrations frequencies in the FTIR spectrum. The observations and results obtained in our work can be used as a reference in order to explain the spectrum of other similar type polyaniline/polysaccharide bio-composite systems for desirable applications. FTIR spectroscopy is an important tool for the quantitative and qualitative analysis of materials, consistency and amount of components in the samples. FTIR is frequently used analytical technique due to its high sensitivity or good detection towards trace amounts of sample and also at the same time it is easy to handle and gives rapid results (Arasi et al 2009; Silverstein et al. 1991). Generally, FTIR spectrum for composite material system seems to be more complicated than that for the pure and single compound. For obtaining a logical explanation of complex FTIR spectrum of a multi-component composite system, the bands in the spectrum can be arbitrarily classified into three main groups viz. bands that appears without

any shifting/change (attributed to groups present in individual component, which does not show any change/interaction during composite formation), slight shifted/overlapped bands (attributed to certain type of interactions, which cause a change in force constant of bonds), appearance of new bands (attributed to the formation of some new identities during material processing).

In the present research, we prepared polyaniline based composites by chemical polymerization of aniline with four different polysaccharides viz. starch (S), carboxymethyl cellulose (CMC), cellulose acetate (CA) and chitosan (CH). These polysaccharides have some certain structural similarities i.e. hydroxyl groups, glycoside linkage and pyranose ring structure, however, they possess different substituted groups. Below we have discussed some interesting and valuable findings on polyaniline based composites, but some issues still remain unresolved, and discussions are still open.

4.2. Experimental Section:

4.2.1 Materials:

Aniline (procured from Merck, India Limited) was purified by vacuum distillation and stored in refrigerator prior to use. Ammonium peroxidisulphate (APS) and hydrochloric acid were used as received from Qualigens Fine Chemicals (India). Cellulose acetate was purchased from BDH limited Poole (England), carboxymethyl cellulose was purchased from Loba Chemie (AR grade) and chitosan was purchased from Sisco Research Laboratories Private Limited (SRL). Double distilled water was used for the preparation of all other solutions.

4.2.2 Synthesis of Composite Material:

Polyaniline/polysaccharide based composite materials was synthesized by in-situ polymerization of prior distilled aniline in 0.1 M HCl along with polysaccharide (aniline polysaccharide ratio w : w = 1 : 1). Aqueous dispersion of starch, CC, CA and CH were used. APS as oxidizing agent was added dropwise into the reaction mixture to initiate the polymerization. For obtaining the best yield we have used, according to stoichiometry, the molar ratio of aniline to oxidizing agent equal to 1: 1.25 (Gautam et al. 2017). Finally, reaction mixture consists of 1 ml aniline, 3.125 mg oxidizing agent, 1 gm polysaccharide in 200 ml of 0.1 M HCl. The reaction mixture was kept under continuous stirring for 2 h at temperature less than 4°C and then kept in a refrigerator for 24 h for completion of polymerization. The product was filtered, washed three times with 0.1 M HCl followed by finally washing with acetone. The materials were dried at 50^{o}C in an oven for 24 h and kept in desiccator.

4.2.3 Instrumentation:

FTIR spectra of PANI and different Polysaccharides were investigated by the Perkin Elmer Spectrum Version 10.03.05 with a range of 4000-400 cm^{-1}. Measurements of the powdered samples were performed ex-situ in the transmission mode with KBr pellet at room temperature. In the FTIR spectra, the x-axis represents the wavenumber (cm^{-1}) and the y-axis the light transmittance through the sample.

A simple weight measurement of the product and reactant give the yield of the composite. We have calculated the percentages of polysaccharide in the composite material as reported elsewere (Ahmed et al. 2004). Another set of experiments was carried out to understand the effect of acid and oxidizing agent on the polysaccharides. The fraction of

polysaccharide degraded by the action of the reaction mixture was calculated by measuring its weight before and after treatment with dilute HCl and mixture of dilute HCl and an oxidizing agent.

Scanning Electron Microscope (SEM) observations were performed using Quanta 200 Company- FEI of USA (SEA) PTE Ltd., Singapore at suitable voltages and magnifications.

The Optical absorption spectrum was measured using Varian Carry 100 Bio dual beam Spectrophotometer, in the wavelength region 200 to 900 nm with a scanning rate 400 nm/min.

Electrochemical experiments were carried out with Model 600D Series Electrochemical Analyzer/Workstation, CH instruments, USA. Composite material modified carbon paste capillary electrode was used as the working electrode, a Pt wire as the auxiliary electrode and an Ag/AgCl (saturated 3M KCl) as the reference electrode. Electrochemical characterization was performed by an electrochemical workstation CHI 660D (CH Instrument, USA) in a three electrode cell configuration with a working volume of 10 ml of 0.1M HCl and of PBS buffer (pH=7) equipped with composite modified electrode as working electrode, Ag/AgCl as reference electrode and a Platinum wire as counter electrode.

4.3 Result and Discussion:

4.3.1 Mechanism of the Composite Formation:

The mechanism of aniline polymerization is reported in the literature (Ahmed et al. 2004; Ghatak et al. 2010). Oxidation of aniline in an acidic medium by oxidizing agent gives macromolecules of protonated conducting form of PANI:

$$Ph–NH_3^+Cl^- + S_2O_8^{2-} \rightarrow -[–Ph–NH–Ph–NH^{\bullet+}(Cl^-)–]_{n-} + SO_4^{2-}$$

The main parameters that affect the nature and molecular structure of the resulting material are initial acidity and the acidity profile, nature of the medium, concentration of the oxidant, duration of the reaction and the temperature (Sapurina et al. 2008; Moiseev et al. 1976). In the composite formation, three different phenomena are taking place simultaneously: interaction of PANI and polysaccharide, partly degradation of polysaccharide due to hydrolysis and formation of PANI.

Glycoside bonds may have different strength in different polysaccharides. Terminal glycoside bonds are more reactive and may result in higher degradation rate because sugar residue at an end of a polymeric molecule requires lower free energy than for an internal unit. Thus, the three types of glycoside bonds i.e. internal, terminal and weak bonds have different reactivity.

4.3.2 Comparative Analysis of FTIR Spectra:

We have compared the spectrum of native and treated polysaccharides, composite materials and its constituents. Interpretation and assignment have been summarized in Table 4.1 and figs. 4.1- 4.3. FTIR spectra of native and treated starch have characteristic bands at 3394, 2903, 1644, 1436, 1153, 1350-1450, 1240, 1130 cm^{-1} (shown in fig. 1A), similar as reported earlier (Zeng et al. 2011). Starch is composed of two types of polysaccharides i.e. amylose and amylopectin. Amylose has interconnected glucose molecules (mostly linear chain and few branched chain) via R-1, 4 glycosidic linkages, whereas amylopectin is interconnected large branched polymer with linkages of R-1,4 in backbone structure and R-1,6 bridges at the branching points.

Strong and broad band at 3000–3369 cm^{-1} represent the –OH stretching or trapped water molecules. Band near 1644 cm^{-1} is ascribed to the adsorbed water and –OH as reported by previous researchers. The bands at 1436 and 1300 cm^{-1} of pristine starch are attributed to the angular deformation of C–H. The bands at 1163 and 1004 cm^{-1} are attributed to CH_2 bending and CH_2 deformation (Sapurina et al. 2011). Stong bands at 997–1130 cm^{-1} represent C-O bond stretch in C-O-C stretch and C-O-H bending (glycosidic linkage) Pawlak et al. 2003. The absorption bands at 775 cm^{-1} and 580 cm^{-1} are attributed to skeletal modes of pyranose rings in the glucose unit (Basavaraja et al. 2012). Two significant differences between treated and native starch are exhibited in appearance of weak band around 1700 cm^{-1} attributed to conversion of some -OH functionality into carbonyl group or presence of certain open chain structure glucose unit (produced due to oxidation) and in decrease in intensity of the band at 1644 cm^{-1} after treatment of oxidizing agent and acid. It may be attributed to the decrease in the amount of adsorbed water molecule (Chiem et al. 2008).

A large number of research articles are available which provide us brief description about the details of characteristic bands of PANI (Kostic et al. 1992; Zareh et al. 2011; Zeng et al. 2011).

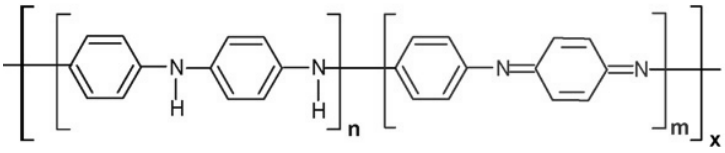

FTIR spectrum of PANI is given on fig. 2. A band around at 3400 cm^{-1} is attributed for the N–H stretching, weak band about 3200 cm^{-1} for OH stretching of physically adsorbed water molecules over the PANI backbone and a medium strong band 2900-3100 cm^{-1} for CH stretching. The spectrum contains bands in the region 1000 to 1600 cm^{-1}: the bands at 1477

and 1573 cm^{-1} exhibit presence of benzenoid and quinoid ring vibration and indicate the partially oxidized state of PANI, i.e. Emeraldine salt form. The medium strong band at 1670-1630 cm^{-1} is attributed to the vibration bands of water molecules (corresponds to humidity during measurement). The bands at 1305 cm^{-1} correspond to C-N/C=N due to the conducting form of the PANI and also due to CH ring in-plane bend, sharp and strong bands at around 1130 cm^{-1} are due to N=Q=N (Q is a quinoid), and at 1240 cm^{-1} due to CCC ring in-plane deformation.

The comparison of FTIR spectra of PANI, starch and PANI/S composite (figs. 4.1, 4.2) reveals the presence of characteristic absorption bands of pure components in the spectrum of a composite. There is a possible interaction between the –NH group of PANI and -CH_2OH group of starch as reported earlier.

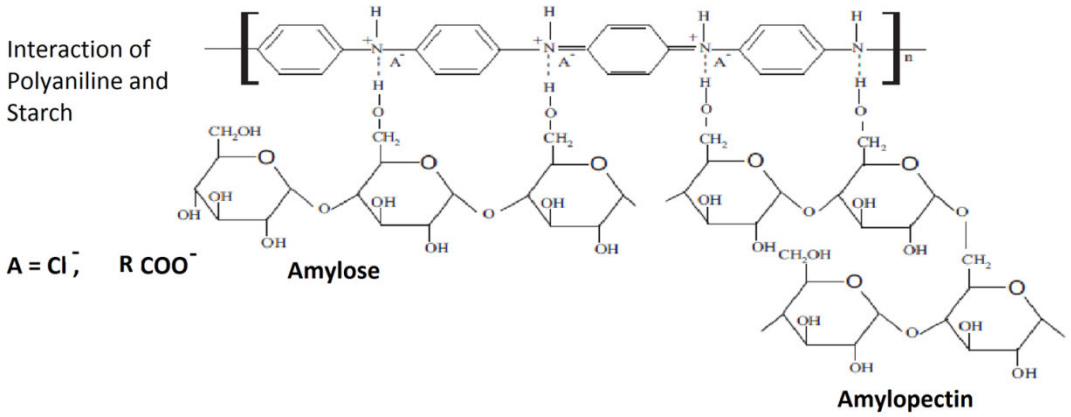

The broad band (3200-3700 cm^{-1}) was assigned to the stretching of the -OH group (inter and intra-molecular hydrogen bonding of polymeric compounds) and NH stretch. Common band at 2911cm^{-1} is due to C-H stretching (appears in all three spectra). The strong absorption bands at 1579 cm^{-1} and 1467 cm^{-1} are attributed to C=C stretching in the quinoid ring and benzenoid structure (NH in-plane bend; CH ring in-plane bend) of the Emeraldine

form of PANI. The intensity ratio of quinoid to benzenoid bands is less for the composite system indicating a more stabilized form of nano-composite with lower conductivity. The band at 1305 cm^{-1} is attributed to C-N, C=N stretching vibration with aromatic conjugation. The characteristic band at 1648 cm^{-1} of starch have lower intensity in the composite material because there are strong interactions of physically adsorbed water and OH group of starch and PANI fiber via weak hydrogen bonding. It is also a notable fact that the intensity of strong band at 3379 cm^{-1} due to OH group present is starch also decreases, while formation of composite system.

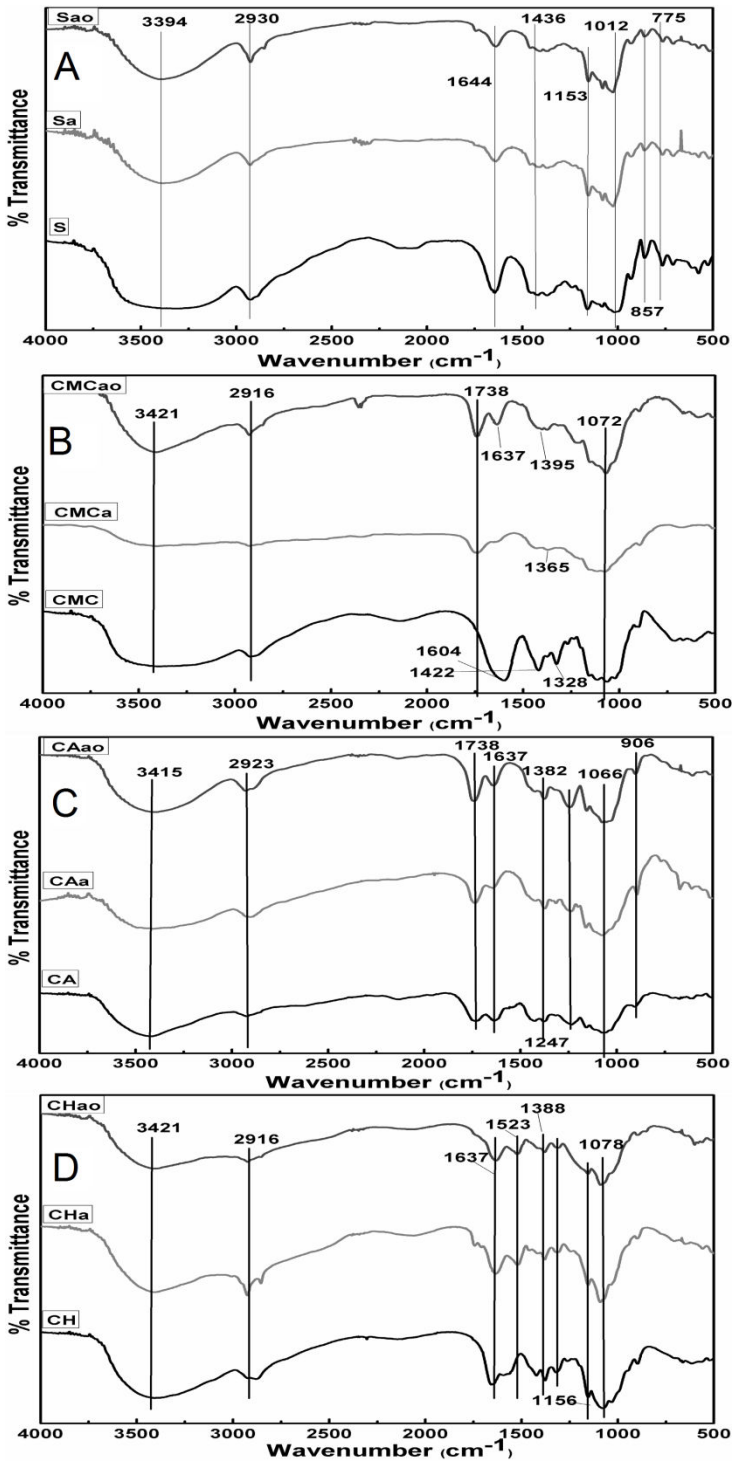

Fig. 4.1 Comparative spectra for native and treated polysaccharides: (A) starch, (B) carboxyl methyl cellulose, (C) cellulose acetate and (D) chitosan

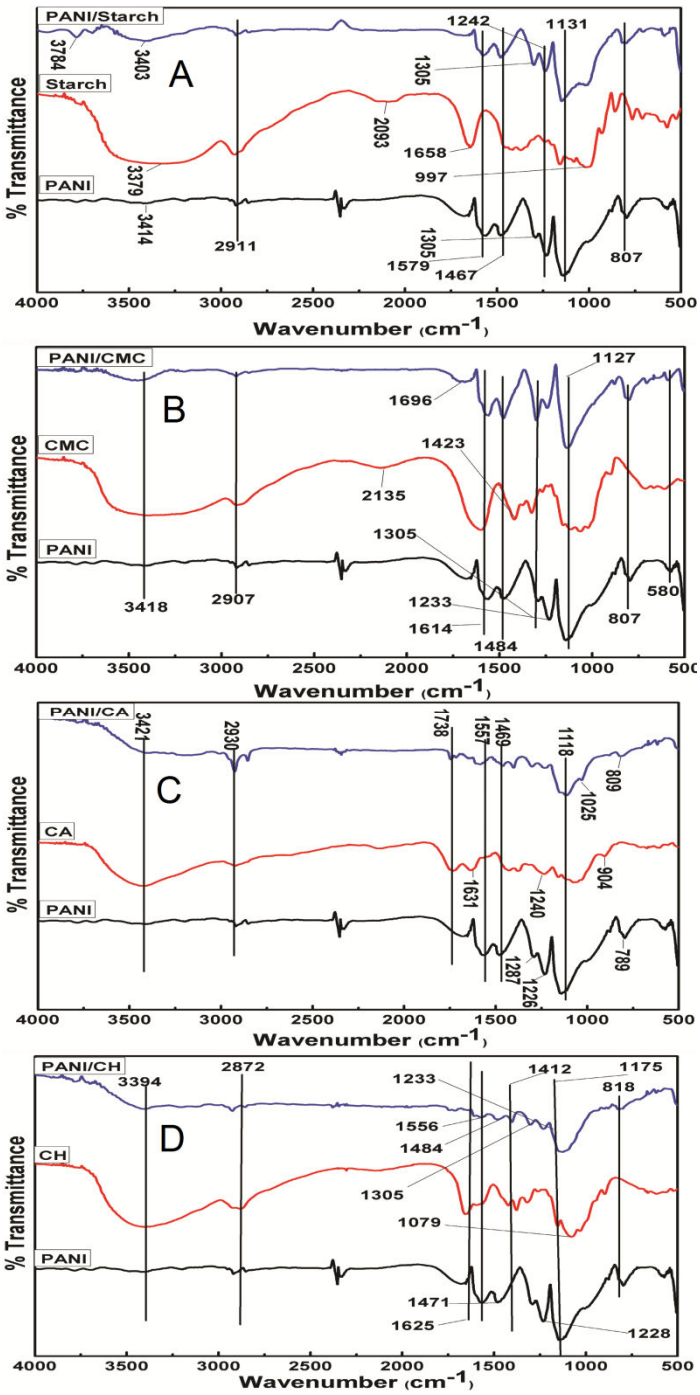

Fig. 4.2 Comparative FTIR spectrum (A) PANI, S and PANI/S (B) PANI, CMC and PANI/CMC (C) PANI, CA and PANI/CA (D) PANI, CH and PANI/CH

Carboxymethyl cellulose contains carboxymethyl (-CH_2-CO-COOH) substituted glucopyranose backbone:

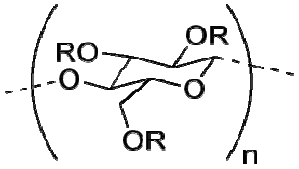

R = H or CH_2CO_2H

FTIR spectra of native and acid/oxidizing agent treated CMC is (fig. 4.1B) reveal the presence of characteristic absorption bands around 3400, 2900, 1600, 1400, 1300, 1100, 702 cm^{-1} (Wang et al. 2005; Peng et al. 2012; Qaiser et al. 2011). Strong band at 3421 cm^{-1} is ascribed to the O-H stretching, weak band at 2916 cm^{-1} – to CH stretching, strong band at 1604 cm^{-1} – to carbonyl/ether group, 1422 cm^{-1} -C-H stretching of -CH_2 group, the alcohol -C-OH stretch (1200 cm^{-1}), strong band around 1072 cm^{-1} can be ascribed to C-O-C structure (ether linkage) from the glycosidic units. The weak band observed between 650-700 cm^{-1} due to ring stretching and ring deformation of α-D-(1-4) and α-D-(1-6) linkage. There is a significant the difference in the spectra of non-treated and treated CMC at 3421, 1604, 1422 and 1072 cm^{-1}. Formation of COOH group is confirmed from decrease in the intensity of the band at 1600 cm^{-1} and appearance of the band at 1738 cm^{-1} for CMC_{ao} due to oxidation of COR group into COOH group. The sharpness of band increases but lesser broadening at 3421cm^{-1} may be due to the decrease in amount of randomly adsorbed water molecule and intermolecular hydrogen bonding.

Composite material PANI/CMC shows characteristic bands related to PANI and CMC (fig. 4.2B) (Pawlak et al. 2003). Active groups (NH_2^+) of the PANI molecules would be involved in strong interactions with carboxylic group of CMC so we observed very weak

absorption band at 3403 cm^{-1} in the PANI/CMC composite material. There are more -OH groups present in the composite materials than its individual components. In the FTIR spectra of composite we observed appearance/disappearance/shifting of some bands: a new band at 800 cm^{-1}, band at 1602 cm^{-1} of CMC disappears and a weak band at 1700 cm^{-1} is ascribed to the carboxylic group present in oxidized CMC molecule. The observation confirms that PANI/CMC composite has integrated structure and there is amide linkage between PANI and CMC. Decrease in intensity for a band at 1300 cm^{-1} is attributed to NH and increase in the intensity of the band at 1230 cm^{-1} is attributed for C-C-C ring deformation that clearly indicates that there is the formation of the integrated composite system.

In FTIR spectra of native and treated cellulose acetate (fig. 4.1C) we observed bands corresponding to frequencies at 3415, 2923, 1738, 1637, 1426, 1382, 1234, 1066 cm^{-1} as reported earlier (Kostic et al 1992; Kamal et al 2014). Cellulose acetate has following structure;

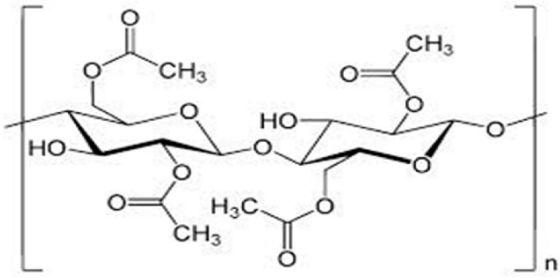

Composite material based on PANI/CA has been extensively characterized and shows the application in membrane formation (Moiseev et al. 1976; Huang et al. 1993). The FTIR spectra of PANI/CA composite material shows a remarkable decrease in intensities of many characteristic bands comparing to the spectra of its constituents (fig. 4.2C). Characteristic bands were observed at frequencies 3786, 2911, 2315, 1727, 1602, 1492, 1102, 977, 573 and

475 cm^{-1}. There is strong interaction between the carboxylic group of CA and NH group of PANI. The strong band at around 1066 cm^{-1} can be ascribed to C-O-C structure (ether linkage) corresponding to glycosidic units (Huang et al. 1993).

The absorption bands in the FTIR spectra for native and treated chitosan are given in fig. 1D:

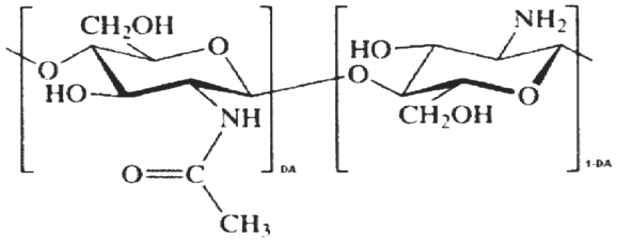

We observed certain characteristic absorption bands around 3421, 2916, 1637, 1523, 1388, 1315, 1230, 1078, 896 and 609 cm^{-1} as reported earlier (Sedaghat et al. 2014). The wide band, which is observed in the region from 3100 to 3500 cm^{-1}, is due to the overlapping between OH and NH stretching vibrations. Aliphatic C-H stretching vibration involvement of amino group is expected at 2968 cm^{-1}. The medium strong band at 1637 cm^{-1} and strong band around 1078 cm^{-1} are attributed to COC (ether linkage) due to glycosidic linkage and a shoulder band at 1619 cm^{-1} is attributed to the NH of primary amine, bands at 1523 cm^{-1} and 1388 cm^{-1} are assigned to the CH_2 bending. A weak band at around 1230 cm^{-1} is attributed to C-N stretch.

In PANI/CH composite material absorption bands at frequencies 3394, 2872, 1625, 1556, 1484, 1471, 1412, 1305, 1233, 1228, 1175, 818 cm^{-1} correspond to the certain corresponding bands of PANI and chitosan. A remarkable fact observed here that most of the bands in FTIR spectrum of composite material have comparatively lower intensity than constitutes components. Medium bands at 1160 cm^{-1} are due to merging of bands at 1175 and 1078 cm^{-1}, attributed to N=Q=N like electronic like the transition of PANI and to glycosidic

linkage respectively. Many bands which referred to chitosan and PANI show shift/merge/disappear in the combined state, which strongly supports the fact that there is a formation of integrated composite system; however, discussion is still open.

As was mentioned above, protonated and deprotonated forms of PANI differ in their spectra. We concentrated on those frequencies of PANI composites, which show significant variation from the calculated value of Leucoemeraldine form of PANI (as reported earlier by R. Kostic et al.) and pure form of PANI (experimentally prepared by us). Important bands are summarized in Table 4.1 and comparison of spectrum has been presented in fig. 4.3.

Spectra of PANI/CA and PANI/CH have comparatively weak signals with lesser intensity indicating that the composite material has higher density, integrated and compact morphology (see below). Presence of weak band at around 1742 and 1748 cm^{-1} indicate amide linkage, which is not present in PANI/S and PANI/CMC. A significant difference observed in the band position and intensity at frequency around 1100 cm^{-1}, which is attributed to the electronic like transition of -N=Q=N-. Redshift of the band position indicates that there is greater charge delocalization through conjugated system of PANI; as a result, one should expect higher bulk conductivity of the material. The sharp band was observed at 1148 cm^{-1} for PANI/S, 1134 cm^{-1} for PANI/CMC, 1107 cm^{-1} for PANI/CA and 1126 cm^{-1} for PANI/CH, from which we can understand the conductivity behavior of the materials. PANI/CA has highest charge delocalization (also confirmed by UV-Visible spectroscopy*)*.

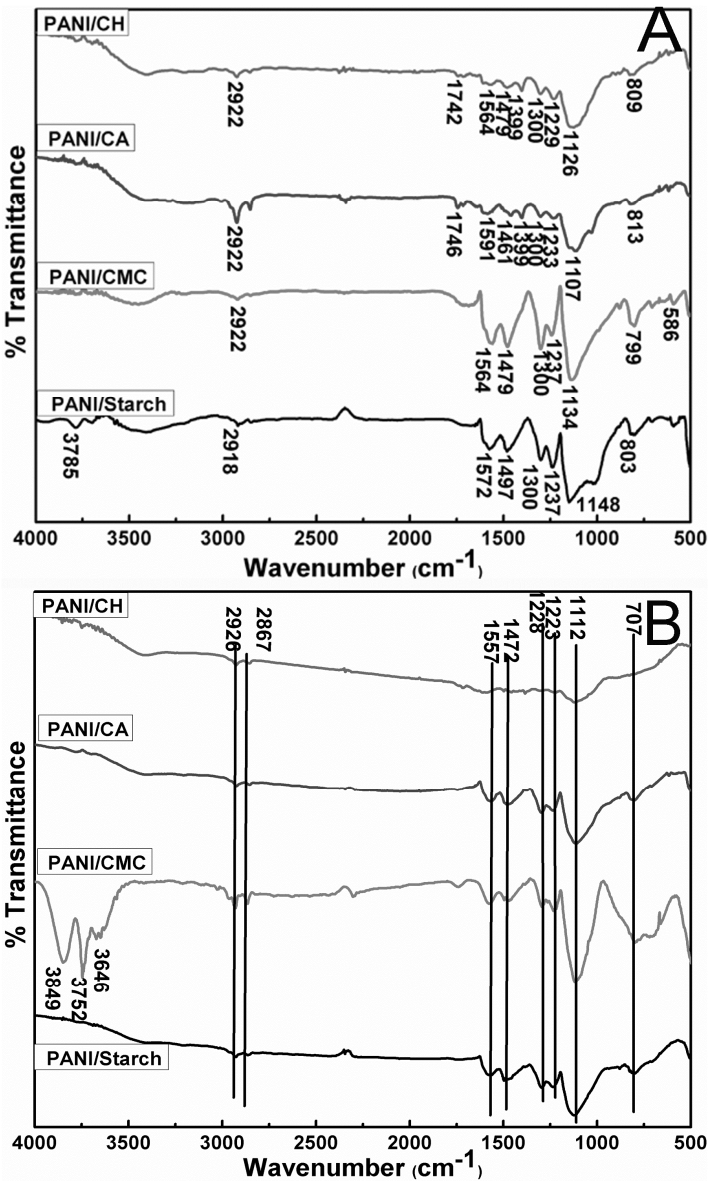

Fig. 4.3 Comparative FTIR spectrum of composites PANI/S, PANI/CMC, PANI/CA and PANI/CH in protonated (A) and deprotonated forms (B)

Table 4.1 Important FTIR frequencies and their interpretation for studied systems

PANI	S	PANI/ S	CMC	PANI / CMC	CA	PANI/ CA	CH	PANI / CH	Calculated Frequencies (cm^{-1}) R. Kostic et al.	Forms of vibrations in Leucoemaraldine form of Polyaniline
-	-	3786, 3690	-	-	-	3786	-	-		
3411	3311	3396	3359	3403	3426		3388	-	3380	NH stretch (vs)
2918	2925	2918	2918	2918	2926	2911	2874	2911	3060	CH stretch (s)
-	-	-	-	-	1734	1746	-	1742		
1675	1646	-	1602	-	1639	1602	1653	-	1630 1615	CC stretch; CH ring in-plane bend (w) (ms)
1573	-	1580	-	1550	-	-	-	1573	1560-1535	CH ring in-plane bend; NH in-plane bend (s)
1477	1420	1484	1418	1477	1426	1492	1426	1484	1450-1475	NH in-plane bend; CH ring in-plane bend (ms)
1300	1367	1300	1300	1300	1374	-	1374, 1315	1300	1320-1300	CH ring in-plane bend; NH in-plane bend; (vw) NH out-of-plane bend; CN strength; CC stretch (vw)
1227	-	1234	-	1241	1234	-	-	1234	1255	CCC ring in-plane deformation; CN stretch
1139	1163	1153	-	1134	-	1107	-	1126	1085	CH ring in-plane bend; NH out-of-plane bend; CCN bend (ms)
-	1004	1006	1058	-	1073	977	1080	992	1020	CH ring in-plane bend; CCC ring in-plane (vw)
793	762	815	712	800	896		896	822	900-810	NH out-of-plane bend (vw)
580	580	587	602	594	609	573	-	-587	575-565	CCC ring in-plane deformation; CNC breathing (ms)

It is an established fact that proton influences the FTIR spectrum of polyaniline. To understand the molecular structure, composite materials were deprotonated with an alkali solution and their spectra were compared (fig. 4.3B). Certain important bands for protonated form disappeared in the base form, indicating variation in B/Q ratio in PANI/S composite. A band around 1000 cm^{-1} disappears in all composites and a common band is observed at 1112 cm^{-1}. Some strong band around 3499 cm^{-1} appears, attributed to hydrogen bonding, in $PANI_d$/CMC composite, whereas weak bands in $PANI_d$/S composite disappear. Many weak bands in the $PANI_d$/CA and $PANI_d$/CH composites either have reduced intensity or disappeared. We can conclude that the composite material has certain weak bonds, which are broken in alkali or in other deprotonated conditions.

4.3.3 Gravimetric Analysis of Composite Materials:

The mechanism of the process and products yields depends on the polysaccharide structure, size of degraded fragments and extent of specific interactions between polysaccharide and polyaniline. Polysaccharides and the degraded fragments are structurally different as a result that dissimilar amount of polysaccharide integrated with PANI in a composite system, however, the same amount of aniline and polysaccharides were used initially. We observe that different polysaccharides have the different degree of hydrolytic degradation in presence of acid and acid/oxidizing agent as a result different fraction of soluble or lower molecular weight fragment present in the solution (Table 4.2).

There are two possible fates of these small molecular fragments either they pass through pores of filter paper washing process or they diffuse deep inside the dwelling space in the polyaniline polymeric matrix and are strongly bind with PANI. To understand the

process of composite formation a simple gravimetric analysis in three different sets of experiment has been carried out. There is a close relationship between the yield of the product, hydrolytically degraded product of polysaccharide with the action of acid and acid/oxidizing agent and the ratio of PANI and polysaccharide in the composite material. In case of PANI/S composite, 13.9 % of starch degrades as small molecular fragments and most of them interact with PANI, so we get a higher yield of 91% and we observe higher ratio of polysaccharide in composite (62.63 %) than fraction of PANI (37%).

In case PANI/CMC and PANI/CA, the yields were 75% and 78%. The extent of cellulosic material shows higher degradation (23.6% and 26.5%) than starch (13.9%) so we observe that percentage of CMC and CA (56.41% and 54.66%) are lower than that of starch (62.6%). Percentage of PANI is higher (43.59 % for PANI/CMC and 45.34% for PANI/CA). It is to be noted that CA has higher degradation as well as higher yield than CMC. On the other hand, we observe CMC degrade into very small size fragments and probably they pass out during the filtration process. In case of chitosan-based composite, it has lower degradation (14%) but lower yield (72%). It can be explained by assuming that small fragments, which does not have strong interaction with PANI, passed out during filtration and washing process; as a result, we observed a comparatively lower yield for PANI/CH than for other composites.

Table 4.2 Result of gravimetric analysis of PANI/polysaccharide composites

Sample	Product Yield (%)	% Wt. loss (acid)	% Wt. loss (acid/O.A)	% of polysaccharide in sample	% of PANI in sample
PANI	68	-	-	0	100
PANI/S	91	12.5	13.9	62.6	37.4

PANI/CMC	75	19.7	23.6	56.4	43.6
PANI/CA	78	19.7	26.5	54.7	45.3
PANI/CH	72	24.2	14	52.8	47.2

4.3.4 UV-Visible Spectroscopic Analysis:

Optical absorptions in the UV-Visible region are associated with the electronic transitions from HOMO to LUMO bands of electronic states. UV-Visible spectroscopy provides valuable information about various levels of oxidation and protonation in PANI. Protonation of the emeraldine base causes a lattice distortion of polyaniline to form a polaronic lattice structure; at higher protonation of emeraldine salt induces the breakdown of the polaronic lattice to a confined bipolaron lattice and; at very high acid strength most of the amine nitrogen become protonated (Huang et al. 1993). A slight change in the confirmation of the PANI may produce significant variation in the spectrum. We have carried out the experiments by making a uniform paste of PANI based composite material with Nuzol oil.

The UV-VIS spectra of the PANI/S, PANI/CMC, PANI/CA and PANI/CH are shown in fig. 4.4. On comparing the four composite material, an interesting arbitrary correlation can be established between fraction of polysaccharide in the composite materials (S=62.63%, CMC=56.41%, CA=54.66%, CH=52.77%) and wavelength for maximum absorption 303 nm (PANI/S), 271 nm (PANI/CMC), 280 nm (PANI/CA), 242 nm (PANI/CH). With the increase in the fraction of polysaccharide within the composite material, peak at maximum absorption shifted towards higher wavelength. It indicates that there is decrease in the binding energy and easiness of charge delocalization. During doping process, neutral polymer backbone converts to a charged π-conjugated system and electrons can through conduction bands. As

an established fact, medium sharp and intense band peak at ~ 450 nm was attributed to the polaron and bipolaron band transitions, (a characteristic of protonated PANI). So, it is confirmed that protonated form of PANI is present in all studied composites, but with a variable degree of protonation. Polaron-π* and π-π* transition bands of the PANI/Polysaccharide composite shifted to longer wavelengths than pure PANI, indicating the interaction between the two components.

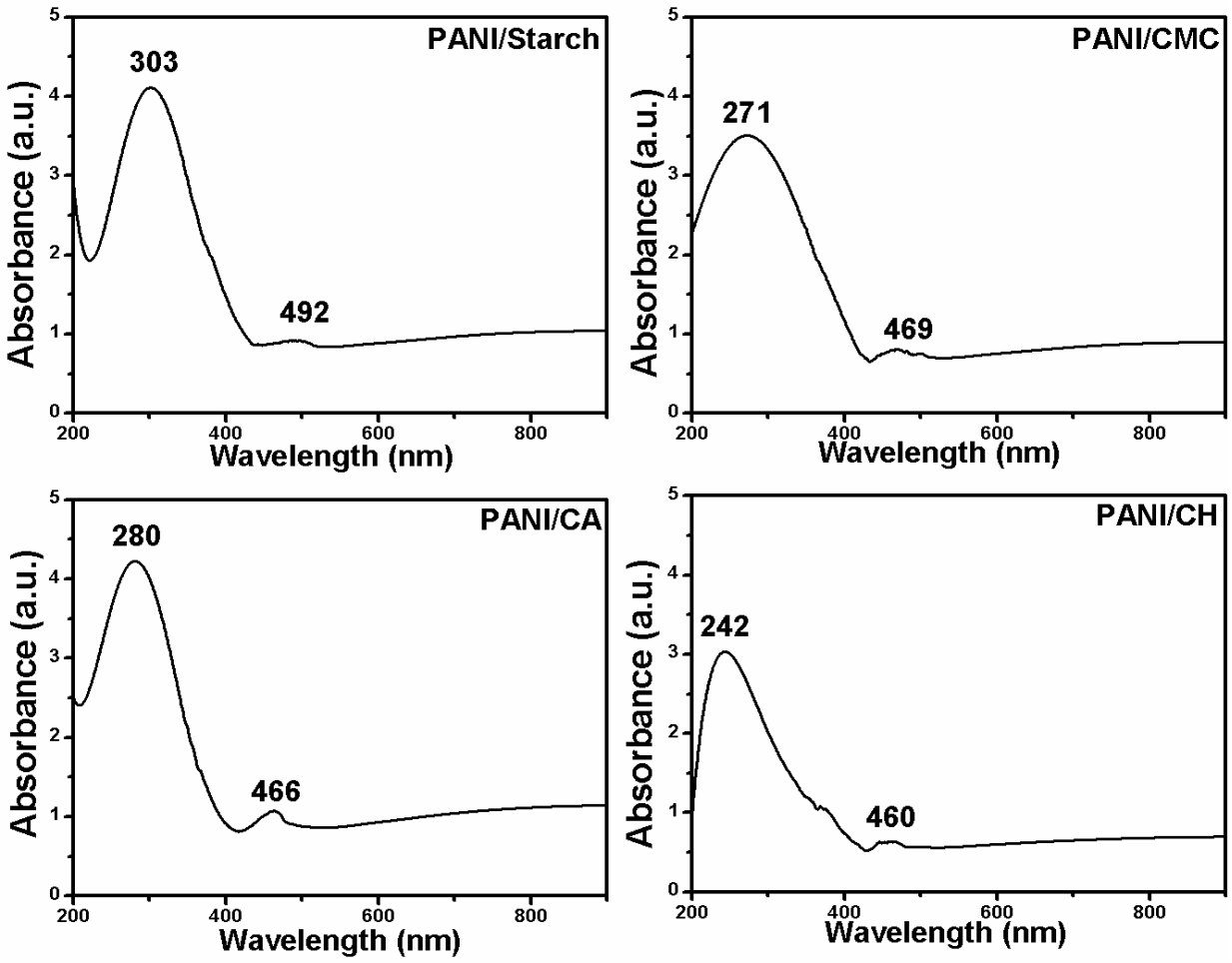

Fig. 4.4 UV-Visible spectra of PANI/S, PANI/CMC, PANI/CA and PANI/CH

Polymers with conjugated π-electron backbones have low energy optical transitions, low ionization potentials and high electron affinities. Dopant affects the conductivity, mechanism of conduction and the band gap. UV spectrum has been used to determine the optical band gap of the composites. The band gap energy was found to be 3.1 eV for PANI/S, 3.0 eV for PANI/CMC, 3.3 eV for PANI/CA, and 3.6eV for PANI/CH. The increase in band gap energy can be attributed to shortening the π-conjugation length of the molecules.

4.3.5 Morphological Studies:

Figure 4.5 shows the SEM images (at low resolution) of PANI/S, PANI/CMC, PANI/CA and PANI/CH, we infer that all composites has rough and porous surface.

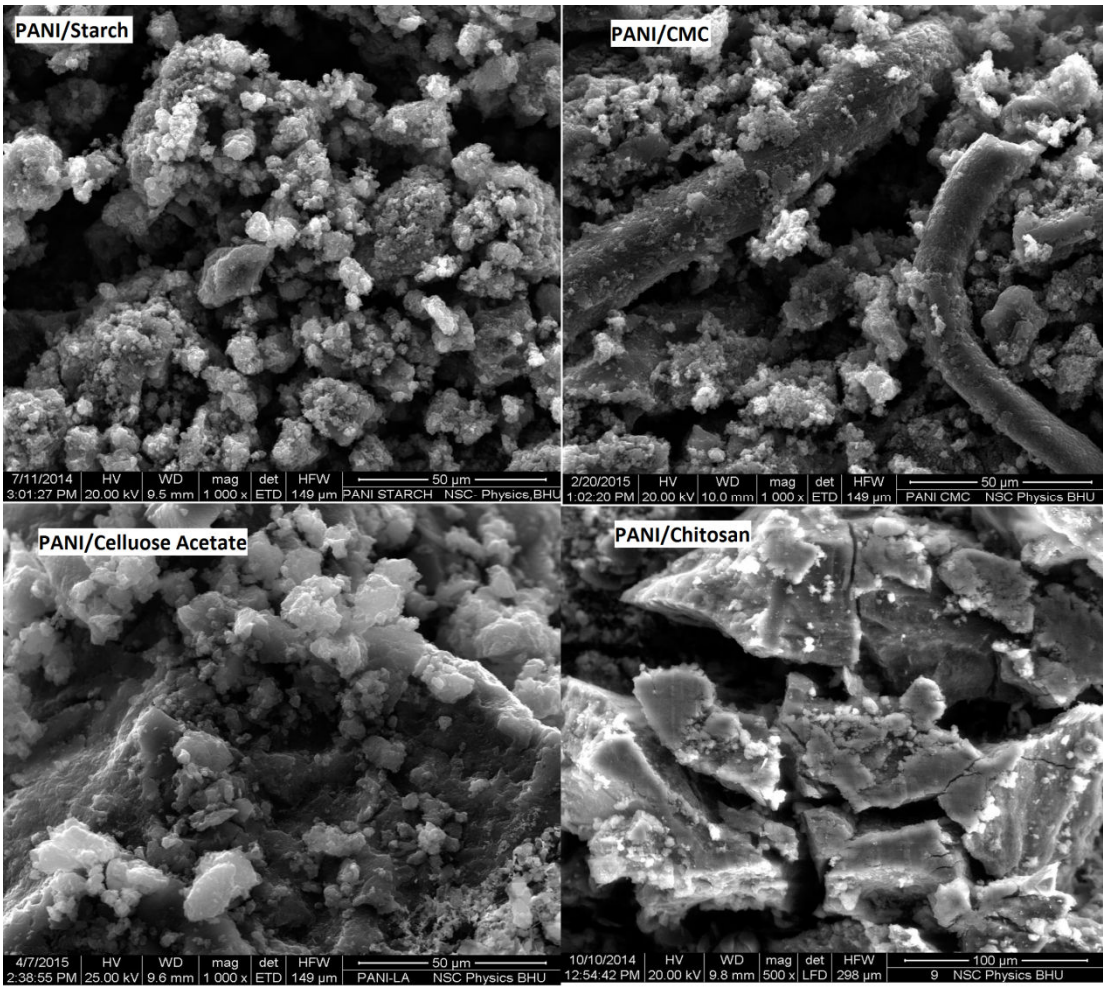

Fig. 4.5 SEM images of PANI/S, PANI/CMC, PANI/CA and PANI/CH

Starch based material has particles of smaller size, aggregation of small globular structures and large inter-granular spacing. CMC molecules have rod-like (or ribbon-shaped) structure, which was degraded into smaller fragments during the composite formation, confirmed from SEM image. PANI layers were coated with CMC fibers. PANI/CA and PANI/CH have compact, less porous integrated morphology indicating strong interaction of PANI with cellulose acetate and chitosan as expected from FTIR spectra.

4.3.6 Electrochemical Studies:

The electrochemical analysis was carried out in order to explore the suitability of composite system as an electrode material and their redox behavior. The cyclic voltammograms (CVs) of PANI/S, PANI/CMC, PANI/CA and PANI/CH, in 0.1M HCl, and in 0.1 M PBS buffer solution (pH=7) at different scan rates are given on fig. 4.6. Mechanism of electrochemical reactions taking place on the electrode can be understood from the scan rate and peak current. We observed that there is an increase in the current response with the increase of scan rate indicating that the conductivity of the surface of the electrode gradually increased with scan rate. To reduce the effects of background current and achieving higher sensitivity low scan rate and smaller electrode cross section should be selected.

Let's analyze the CVs of composites at a scan rate 200 mV/s (fig. 6). The CV displays well defined oxidation-reduction responses indicating that all the prepared materials are electroactive in the solution of higher pH. At pH-7 PANI/S composite shows the highest current response, whereas PANI/CA shows the lowest current response. In 0.1 M HCl, PANI/CH shows highest current response, where as PANI/CMC has lowest current response

among the four studied materials. The higher current response indicates the better conductive and higher surface area of the material. The rate of H^+ ions movement and involvement of electrons transfer process of the composite can be correlated with the peak potential difference.

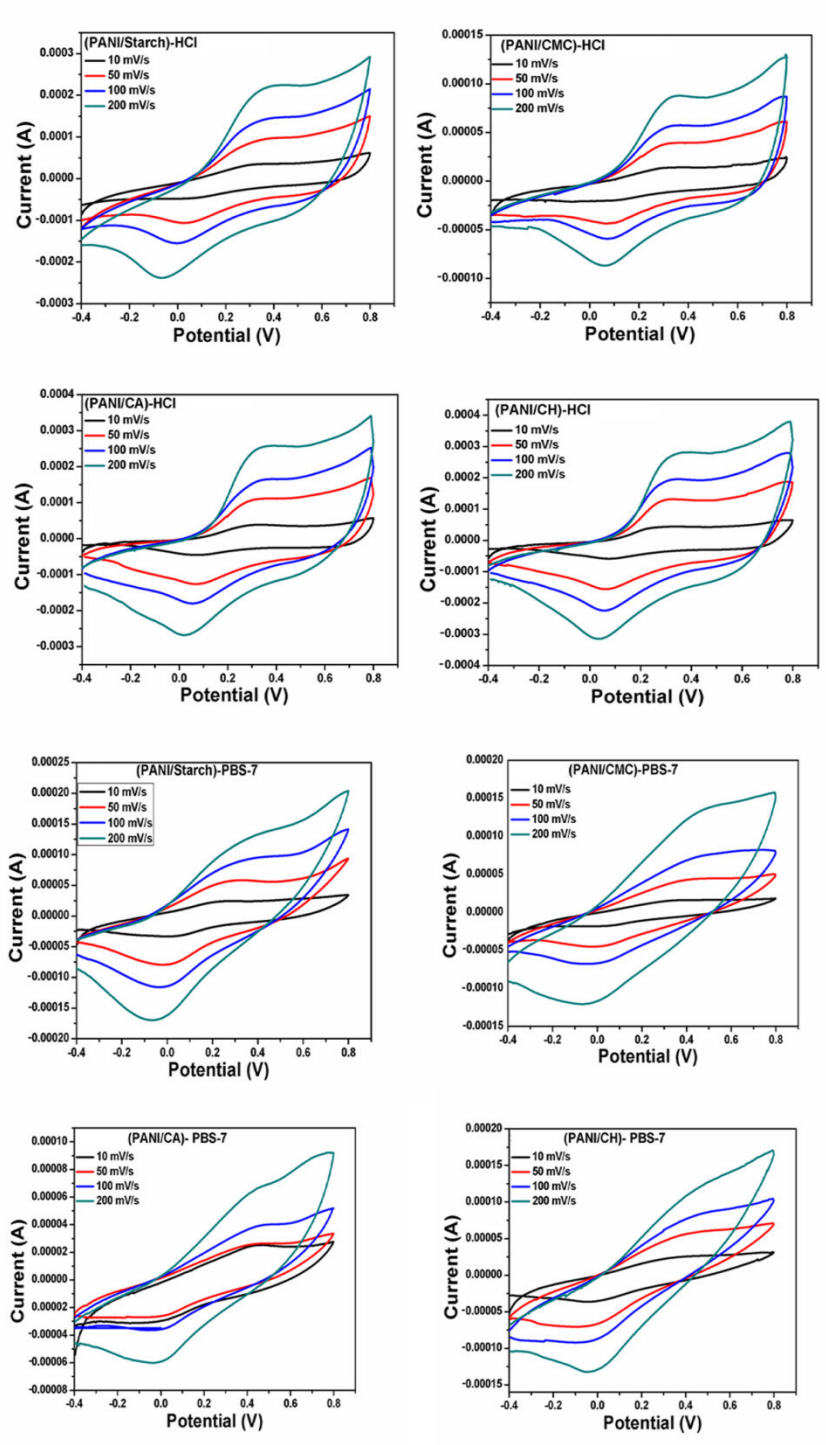

Fig. 4.6 Cyclic voltammogram of PANI/S, PANI/CMC, PANI/CA and PANI/CH in 0.1M HCl and in PBS buffer solution at different scan rate

Larger the peak potential difference indicate slower the charge movement and vice versa. High height of oxidation peak and anodic current are preferred to the faster electron-transfer reaction in the electrochemical system. PANI shows two main redox processes: at lower positive potential ~220 mV it represents the leucoemeraldine (fully reduced form)/emeraldine (half oxidized form) transition, while at higher positive potential ~580 mV it corresponds to emeraldine/pernigraniline (fully oxidized form) transition.

Generally, polysaccharides are not electroactive species but they are able to modify the electrochemical behavior of the composite. The difference in peak potentials is largest in PANI/S system than in others. Generally, the major problem for using PANI as an electrode material is its use at neutral pH, because its electroactivity was lost in the solution of higher pH. So, PANI/polysaccharide-based materials, which exhibit good electro-activity in PBS buffer solution, good dispersion ability, biocompatibility and easy conjugation of biomolecules, porous morphologies, may be promising candidates for enzyme immobilization and other electroanalytical applications. PANI can form strong hydrogen bonds with -OH on the surface of polysaccharide and as a result an integrated composite system is obtained, which provides an ambient environment to biomolecules. Further extensive studies on the electrochemistry and effect of solution pH on the redox behavior of the polyaniline/polysaccharide systems and their applications in the area of sensor/biosensor are under open discussion and will be communicated shortly in our future publication.

4.4 Conclusions:

We conclude from the above discussion that PANI interacts strongly with the polysaccharides. Incorporation of polysaccharides increases the hydrogen bonding and

hydroxyl functionality as a result composite materials have improvement in its biocompatibility, dispersion ability, functionality and solubility. We have observed that different types of polysaccharides may interact with PANI via O-H, COOH functionality. Hydrolytic degradation results in variable degree of soluble or lower molecular weight fragments of polysaccharide.

Although, the same amount of aniline and polysaccharides were taken initially, we observed that yield of composites are significantly different. From SEM images, it was concluded that PANI/S is more porous, where as PANI/CH and PANI/CA has compact morphology. From cyclovoltammogram, we have studied the redox behavior of all the four composites and they show good electro-activity in the solution at pH-7. PANI/S reveals stronger interactions, small size particle with more porous morphology, as a result, there is increased current intensity due to the increased electroactive area.

In this chapter, we have tried to provide a logical explanation for two significant observations viz. difference in product yields and variation in the ratio of PANI and polysaccharide in the composite material although same ratio of starting material was taken initially. The basis for such an interesting consequence is probably attributed to the factors that govern the interactions among particles, morphology and size of the particles, the number of reactive site on the polysaccharide chain, the extent of hydrogen bonding and amount of unreacted aniline monomers. In the conditions, where there is porous morphology/loose structure, size of degraded polysaccharide fragment is small and comparatively stronger interactions between polysaccharide fragment with the polyaniline matrix. The small size fragments diffuse deep inside into the polymeric matrix, and they find

dwelling space there. As a result, we get higher yield and higher fraction of polysaccharide in the composite material.